

# CMB RoPE: A CMB Polarimeter

Asad Aboobaker <sup>1</sup>

Advisor: George F. Smoot <sup>2</sup>

Senior Honors Thesis

Physics Department

*University of California, Berkeley*

May 9, 2000

---

<sup>1</sup>email: asad@uclink4.berkeley.edu

<sup>2</sup>email: gfsmoot@lbl.gov

## **ABSTRACT**

I describe a new experiment designed to measure the polarization of the Cosmic Microwave Background. First, I discuss the origin and importance of CMB polarization. Then I describe various approaches to measuring CMB polarization and the results of previous measurement attempts. Then I describe our experiment in detail and the challenges we have faced in getting the project operational. Finally, I look to the future of our experiment and ways to improve its performance.



classical analogy. Suppose you have an electron sitting at the last scattering surface, with a hot region near it and a cool region  $90^\circ$  away. The (unpolarized) radiation from the hot region causes the electron to oscillate in the vertical direction as well as along the line of sight. The (unpolarized) radiation from the cool region causes the electron to oscillate horizontally and along the line of sight. The oscillation along the line of sight produces no radiation that we can observe, but the vertical and horizontal oscillations each produce polarized radiation in their respective directions. Due to the higher power of radiation received from the hot region, the electron oscillates more in the vertical direction, imparting a very slight linear polarization to the outgoing radiation. In this way, CMB polarization is only sensitive to the local temperature anisotropy quadrupole moment. Most theoretical estimates put the level of polarization at 10% of the anisotropy level — that is, at the  $\mu\text{K}$  level.

## 2. The Importance of CMB Polarization

What will we gain from measuring the level of CMB polarization? First, it is a natural result of cosmological models, and a measurement will be a basic check of the assumptions that go into these models. In addition, polarization measurements can be used to break parameter degeneracies in CMB temperature measurements, providing a complementary set of information. Also, a polarization map can distinguish between various physical conditions that can create temperature variations: scalar (density), vector (vortical), and tensor (gravitational wave). In addition, a polarization measurement at large angular scales is a sensitive probe of the epoch of reionization (star formation) in the Universe.

## 3. Different Approaches to Measuring CMB Polarization and Previous Results

As with most physics problems, there are a number of ways to measure CMB polarization. The simplest method to measure polarization, conceptually, is to use a rotating detector which is only sensitive to one polarization direction. As the detector rotates, the output will be modulated by  $\cos^2 \theta$ . This is the method we use (see Section 5.1). A somewhat similar method is to use an unpolarized receiver (such as a bolometer) and modulate the incoming signal with a filter. This technique is used by CalTech’s Polatron<sup>3</sup> experiment, with a bolometer detector and a quartz half-wave plate operating at mm-wavelengths. Another method is to split the incoming signal into its two polarized components, amplify each one separately, and extract the signal from the difference of the two channels. This method has the advantage that you are observing both polarizations simultaneously, increasing observing efficiency. In schemes such as these, some sort of

---

<sup>3</sup><http://astro.caltech.edu/~lgg/polatron/ppro.html>

modulation is necessary to control systematics, either chopping on the sky (Princeton’s PIQUE<sup>4</sup>), or perhaps rotating the apparatus 90°. Most CMB polarization experiments are ground-based, which allows the long observation times required to detect polarization.

We are not the first to attempt to measure CMB polarization. In fact, Penzias and Wilson determined that the CMB was at least 90% unpolarized. Since then, a number of different groups have attempted to measure polarization, with the upper limits currently at about 20  $\mu$ K. This is an order of magnitude above theoretical estimates for the level of CMB polarization. Now, with a new generation of low-noise HEMT amplifiers, measuring polarization has become a feasible task. No less than five institutions in the U.S. and at least one international collaboration are developing or, in Princeton’s case, running ground-based CMB polarization experiments. All of them cover different frequency ranges and angular scales on the sky, and represent a wide variety of experimental techniques. In addition, of the two upcoming CMB satellites, MAP has a chance at measuring polarization, while Planck Surveyor will undoubtedly do it — if you can wait for 2007.

#### 4. Challenges

Naturally, if this measurement was easy, someone would have already made it. We face a number of experimental challenges to measuring CMB polarization, as well as technical hurdles (see Section 7.1). The first challenge is, of course, the extremely low level of CMB polarization. A  $\mu$ K signal alone is very hard to detect, but on top of that we have to deal with various foregrounds. At 9 GHz, the atmosphere emits at a temperature of a few Kelvins, but the radiation is thought to be unpolarized. Of more concern is galactic synchrotron emission which, at 9 GHz, is not only highly polarized, but also expected to be several orders of magnitude larger than a polarized CMB signal. In addition, dust emission is highly polarized as well, but has negligible emission at 9 GHz.

---

<sup>4</sup><http://dicke.princeton.edu/~pique/pique.html>

## 5. Our Experiment: CMB RoPE

Our experiment is called CMB RoPE (Cosmic Microwave Background ROTating Polarization Experiment). In the following sections I will discuss in detail various facets of the experiment’s design and construction.

### 5.1. Design Overview

CMB RoPE, as mentioned in Section 3, is basically a rotating linearly-polarized detector operating at 9 GHz. We use an offset-axis parabolic dish feeding a scalar horn to collect the radiation, and the entire instrument rotates around the beam axis at 6 RPM (0.1 Hz). The RF signal travels through a cooled first stage amplifier and 2 room-temperature amplifiers and a bandpass filter to a square-law detector. The resulting voltage signal is then amplified further, integrated for  $15^\circ$  of rotation, and sent to the data acquisition system to be bundled with housekeeping data and sent to the computer. The receiver, data acquisition system, and necessary power supplies are mounted on the rotating platform, with a slipring to get power in and signals out. The instrument receives radiation from the zenith, and we use the rotation of the Earth to scan a strip on the sky. We drift-scan the same strip repeatedly to achieve maximum sensitivity.

### 5.2. Optics

The optical design is somewhat unusual, using an 1.8-meter off-axis parabolic dish rather than the more common axially symmetric design. The off-axis design has the advantages of low sidelobes and an unobstructed beam since the receiver is placed to the side of the dish. The feedhorn illuminates the dish with a HPBW of  $35^\circ$ , which gives the entire system an angular resolution of about  $2^\circ$ . The feedhorn is a corrugated scalar-mode design, designed for beam symmetry and low sidelobes. It has a circular aperture 10 cm in diameter, a  $45^\circ$  semi-flare-angle, and a circular waveguide at the base. The circular waveguide is connected to a stepped circular-to-rectangular waveguide transition which also serves as a polarization filter (For more information on the horn, see Sec. 7). The transition then connects to a waveguide-to-coax transition, and an SMA coaxial line carries the signal to the first-stage amplifier.

Surrounding the dish is an aluminum-sheet ground shield. This shield rotates with the dish and ideally prevents radiation from the ground ( $\sim 300$  K) from entering the horn. However, since Berkeley is surrounded by hills and our location at Lawrence Berkeley Lab is in the hills, the horn still has a direct line of sight to the hills for part of its rotation.

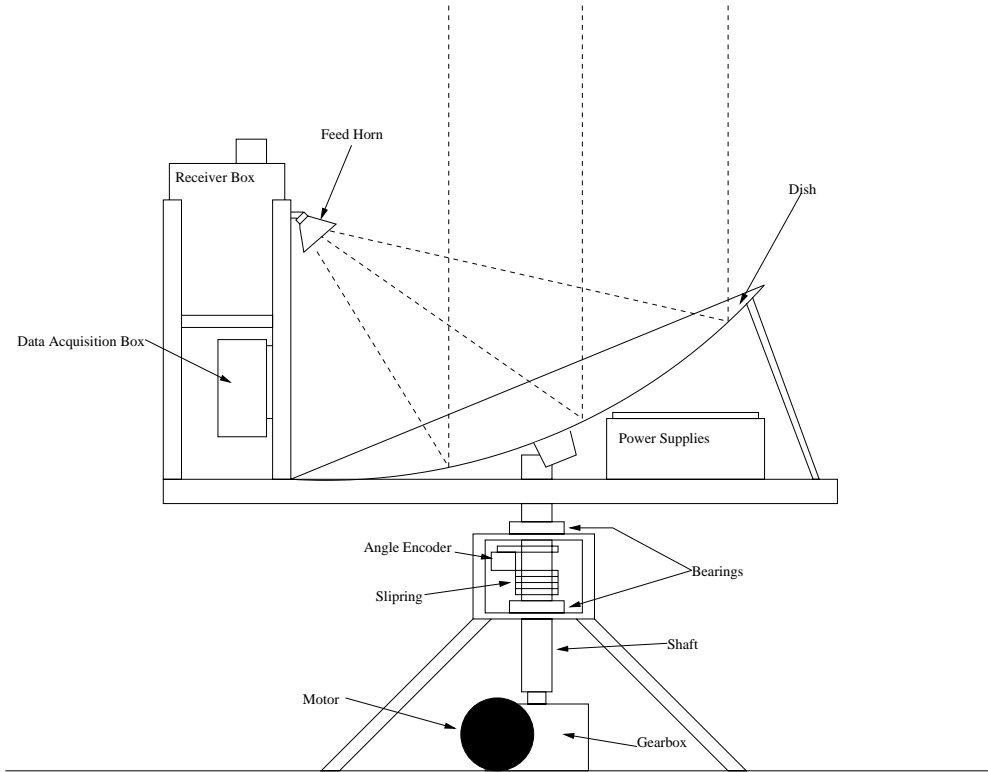


Fig. 2.— CMB RoPE simplified schematic diagram

### 5.3. Signal Chain

The receiver is a simple, direct-gain total-power design (see Fig. 5.3). The signal from the horn goes to our first stage amplifier, made by NRAO. It is a 3-stage HEMT amplifier with a gain of 30 db from 8-10 GHz when cooled to 77K. The amplifier is mounted to a cold plate inside a liquid nitrogen dewar. Under ideal conditions, the LN lasts for >40 hours. However, conditions are rarely ideal (see Section 7.1.1).

From the first stage, the strengthened signal travels to the second and third stage amplifiers. These amplifiers, made by JCA Technology<sup>5</sup>, have gains of 40 db and 20 db, respectively, each rated for 8-12 GHz operation. To reduce out-of-band noise, the signal passes through a TTE 8-10 GHz bandpass filter<sup>6</sup>. The signal then passes through a detector diode which converts incoming power to a voltage. This voltage signal is amplified by a DC amplifier.

The DC amplifier consists of a low-noise instrumentation amplifier front end coupled to a

---

<sup>5</sup><http://www.jcatech.com/>

<sup>6</sup><http://www.tte.com/>

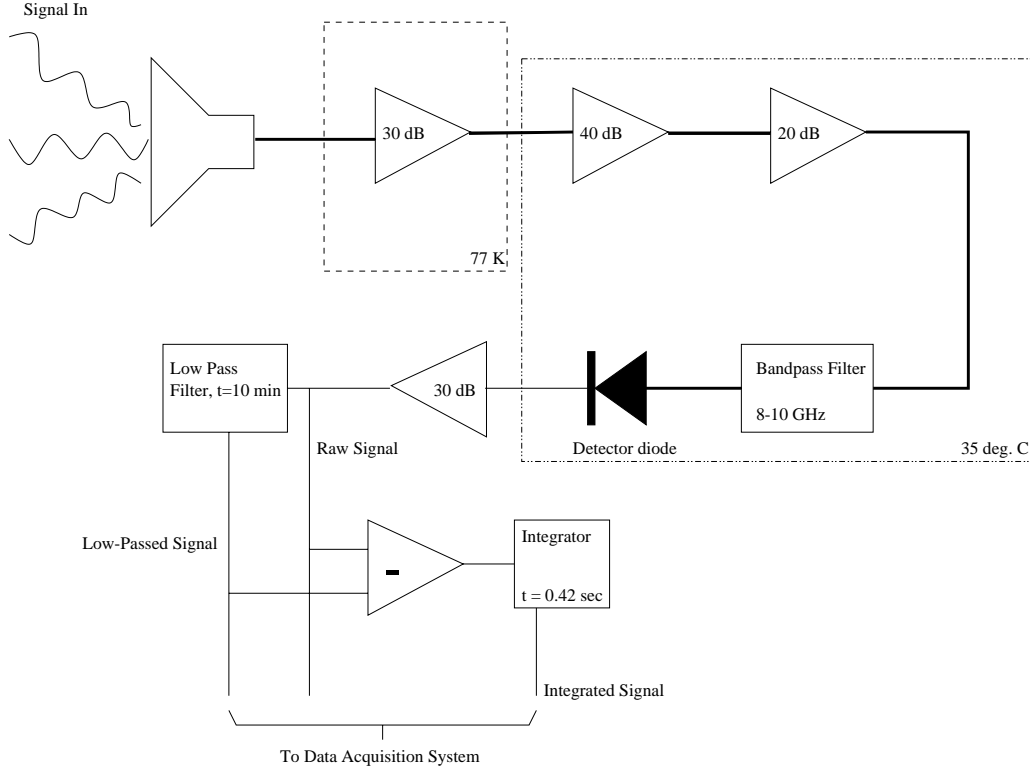


Fig. 3.— Receiver block diagram

low-pass filter with a long (10 minute) time constant. The output of this filter is subtracted from the raw signal to remove the large constant power level while leaving variations at the rotation period (10 seconds) unaffected. The resulting signal is then integrated for 0.42 sec. (15° of rotation) at a time and then sent to the data acquisition system.

The receiver has a system temperature of 80 K when the first stage amp is cooled to 77 K. Our RMS temperature is given by:

$$\Delta T_{RMS} = \frac{T_{sys}}{\sqrt{Bt}} = 1.8 t^{-1/2} mK \quad (5-1)$$

Where  $B$  is the bandwidth (2 GHz) and  $t$  is integration time. Thus, with our sensitivity and the need for  $\Delta T_{RMS} = 5 \mu K$ , this corresponds to  $t = 36$  hours per 2° pixel per polarization. At our latitude of 38°, we have about 140 pixels in one strip on the sky doing a zenith scan. This corresponds to a total observing time of over 400 days in order to reach our desired sensitivity. Even if we could observe 365 days out of the year, data would still have to be excised when the sun is near the beam, and weather makes observing year-round impossible anyway. Thus, this experiment will take a long time.

All RF components are housed in an insulated, thermally controlled box, and the second- and



third-stage amplifiers, filter, and diode are mounted on a thermally-controlled plate inside another insulated box (see Section 5.4 for details on the thermal control).

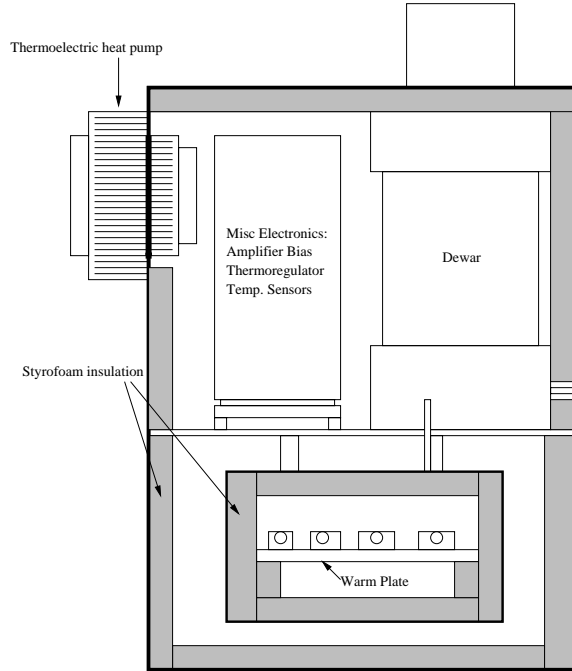


Fig. 4.— Receiver box layout, side view

#### 5.4. Ancillary Electronics

Besides the RF section and data acquisition system, there are various other electronic components in the experiment. Mounted inside the receiver box are an amplifier bias card, a thermoregulator circuit, and two temperature sensor circuits. In the power supply box is another thermoregulator circuit, and a shaft angle encoder is mounted on the drive shaft.

The bias card is supplied by NRAO with their first stage amp. It provides the precise drain voltages and currents for each stage in the amplifier. When set incorrectly, the amplifier oscillates at low frequencies. However, the preferred values were supplied to us by NRAO, so this was not an issue.

The receiver box has 2 stages of thermoregulation. We use a Melcor<sup>7</sup> thermoelectric heat pump to cool or heat the receiver box as needed, connected to the thermoregulator in the power supply box. The thermoregulator is controlled by a thermistor mounted in the Melcor’s heatsink

---

<sup>7</sup><http://www.melcor.com/>

(for minimum phase lag in responding to temperature changes). Using just the Melcor, the air in the box can be regulated to  $20^{\circ}\pm 1^{\circ}$  C easily.

The second stage of thermoregulation controls the temperature of the warm RF components via their aluminum mounting plate. The plate is mounted in its own insulated box inside large box. The thermoregulator uses heating resistors to heat the plate when needed. Since the resistors cannot cool the plate, the temperature is regulated at  $35^{\circ}$  C (i.e. higher than the air surrounding the box) so that shutting off the resistors will let the plate cool. The 2-stage thermoregulator can keep the plate temperature to within  $\pm 0.1^{\circ}$  over a 24-hour period. The power-on behavior exhibits oscillations as the thermoregulator overshoots its desired temperature, but the oscillations damp out within 30 minutes.

In addition to thermoregulation, we also monitor and record the temperatures of various components in the system. We use Analog Devices’ AD590 temperature sensors and their accompanying circuit to measure the temperature of the warm RF plate, the air in the big box, the ambient air temperature, and the feedhorn temperature. We also have a temperature sensor mounted in the dewar. We use a LakeShore Cryotronics<sup>8</sup> cryogenic diode to monitor the temperature of the dewar’s cold plate. This is a quick and easy way to tell when the dewar has boiled off its liquid nitrogen.

Last, we use a an optical encoder to provide shaft angle information as the instrument rotates. We use a CP-350 10-bit absolute position encoder from Hathaway Motion Control<sup>9</sup> which is small, lightweight, and inexpensive. 10 bits ensures better than  $0.5^{\circ}$  precision in the shaft angle. The encoder rotates with the shaft and is driven by a gear which is fixed to the base. This was necessary because the encoder signal is packaged with the rest of the signals into a data frame, and the data acquisition system is mounted on the rotating platform.

## 5.5. Data Acquisition

The data acquisition system (DAS) consists of a control module, an analog multiplexer, a pair of digital inputs, and an RS-232 interface unit. Along with the raw signal, the low-passed signal, and the integrated signal, we supply the analog inputs with the various temperature readings. One of the digital inputs reads the shaft angle, and the other is currently unused. These values are packaged into a single data frame, converted to RS-232, and sent to our PC. The data frame layout is given in Table 5.5.

the table	isn’t here	quite yet
blah	blah	blah

---

<sup>8</sup><http://www.lakeshore.com/>

<sup>9</sup><http://www.opticalencoder.com/>

At the PC, we use software written in National Instruments’ LabVIEW package to read the data frame, display, and record the data. The front end of the data acquisition software displays real-time graphs of all parameters supplied to the DAS: raw, low-passed, and integrated signals, the various temperature readings, and shaft angle.

## 6. Calibration

The typical method for absolute calibration, using beam-filling blackbodies of various temperatures, is difficult to implement with CMB RoPE. An absorber that fills the beam of our telescope would be unreasonably large, and a cold load presents even more problems. A less ideal solution is to use absorber placed in front of only the feedhorn. Unfortunately, this method cannot account for the emissivity of the dish and shielding. CMB RoPE also uses a noise diode for relative calibration. The noise diode radiates via a quarter-wave antenna mounted at the edge of the dish and is activated once every 20 frames. We have calculated the diode to produce a signal of 1 K at the feedhorn, easily detectable with even one sample by our receiver.

### 6.1. Mechanical Design

The feedhorn is mounted at the focus of the off-axis dish on an aluminum tower that I built. The receiver box is mounted behind the feedhorn, and the data acquisition system is mounted directly below in its own box. The tower is mounted on two aluminum beams which coupled to the shaft by an aluminum plate and collar. On the opposite end of the beams, underneath the dish, is the power supply box which also acts to balance the weight of the receiver tower. The rotating platform was built by myself, Mike Leung, and Peter Curran. The dish is supported by an adjustable yoke welded to the shaft and a turnbuckle at the back for precise angle adjustments. The shaft itself is a 2” steel tube with 1/4” thick walls. The aluminum plate rests on a bearing which is attached to a welded steel base. The base, designed and built by Peter Curran and Ian Ellwood, is made from welded steel Uni-Strut and has 1/4” thick steel plates on the load-bearing surfaces. Below the top bearing is the angle encoder and then the slipring to get power in and a digital signal out. Below this is another bearing and then a flexible coupling to attach to the motor. The motor is an industrial electric 240-V, three-phase unit with a worm drive and variable gearbox, and it is easily capable of rotating our apparatus.

## 7. Feedhorn Optimization and Testing

The most focused part of my work was centered on the construction and testing of the feedhorn. The horn was designed by fellow student Ki Won Yoon following a procedure given in [6]. The goals of the design were to have beam symmetry in both polarization axes and low

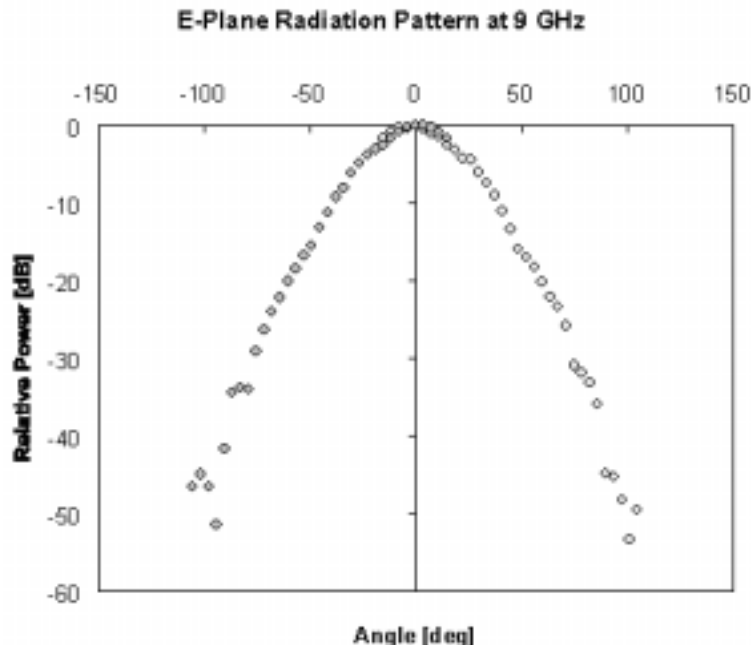


Fig. 5.— This will be a drawing of the feedhorn, once I get the image..

sidelobes. A diagram is shown in Fig. 7. The horn was machined out of two pieces of aluminum, one for the main section and another for the outer quarter-wave trap. The quarter wave trap ring was heat-shrunk on to the horn and secured further with screws.

The original design of the horn called for a quarter-wave probe in the back section of the horn to transfer the signal to the coaxial line. This design worked dismally. We could only achieve return loss (reflected power) figures of  $\sim -10$  dB over the range from 8-10 GHz. I tried a variety of different approaches to remedy this situation. I made a mockup circular waveguide to test these various approaches.

The first thing I tried was inserting metallic objects to induce reflections, hopefully in such a way as to increase the amount of power picked up by the probe. I tried various shapes, such as wedges of various sizes and cones in order to attempt a smooth impedance transition to the probe. These techniques were only successful in producing good ( $-20$  dB) reflection performance in narrow frequency ranges. The next step was to use a movable back wall and try and find the optimum position, which also only worked for a narrow frequency range. The last technique following this course of action was putting tuning screws in the waveguide. The tuning screws and movable back wall together were successful in producing  $-20$  dB return loss in a 1-GHz band anywhere within the 8-10 GHz window. However, at the edges of the band, performance suffered drastically, with reflections as high as  $-5$  dB.



Fig. 6.— An on-axis photo of the feedhorn, showing the outer quarter-wave traps, inner corrugations, and stepped transition. The waveguide-to-coax transition is at the back.

I felt that this approach did not lead to viable solutions. For example, by the end of my testing with the mockup waveguide, it had 10 tuning screws along its length. Not only was it incredibly difficult to tune, but it also would have been difficult to duplicate on the actual horn. Thus, a new approach was in order.

I tested a stepped transition from the 10 GHz GEM receiver that was in our lab. Despite being designed for a slightly higher frequency, I found that this transition worked remarkably well except at the lowest end of our frequency band. Inspired, I machined a similar transition, scaled to our frequency band and waveguide size. It consists of four  $\frac{1}{4}$ -wave-thick stacked plates, the first with a circular waveguide, the rest with rectangular waveguides transitioning to a standard WR-112 rectangular waveguide. When tested with a commercially available WR-112 waveguide-to-coaxial adapter, the new stepped transition worked remarkably well, exceeding my expectations. When tested with a smaller WR-90 waveguide-to-coax adapter, surprisingly, it worked even better. This is the final configuration we use on the horn now. The old waveguide section of the horn was machined off, and the transition was attached.

After the horn was operational, we had to determine the beam pattern. Using a computational

spherical wave expansion, Ki Won calculated the  $-10$  and  $-20$  dB points as  $34^\circ$  and  $54^\circ$  off-axis, respectively. We tested the horn on the roof of Bldg. 50 at LBL, where the L-shape let us test the radiation pattern without reflections in one direction. We set up a transmitter at on the short leg and placed the horn and receiver (sans first-stage amplifier) on a rotating platform on the long leg. As we rotated the horn, we had to increase the power of the transmitter to account for the attenuation of off-axis signals at the feedhorn. We determined the HPBW of the horn to be  $35^\circ$ , and the  $-10$  and  $-20$  dB points to be  $35^\circ$  and  $52^\circ$  (E-plane) and  $40^\circ$  and  $60^\circ$  (H-plane), agreeing well with the theoretical predictions. A plot of the E-plane radiation pattern is shown in Fig. 7. In addition, we se no sidelobes to  $100^\circ$  off-axis.

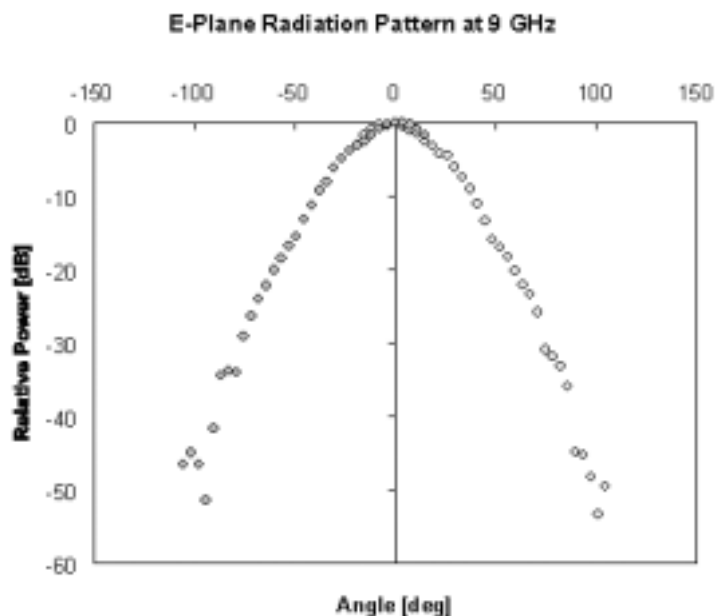


Fig. 7.— E-plane radiation pattern for our feedhorn.

### 7.1. Problems

We currently have no data to show for our efforts in constructing this experiment. As is true for any physics experiment, we have faced numerous problems in our progress. Most of these, from a non-functional amplifier to all manner of noise, have been dealt with satisfactorily. However, a few hurdles still remain before “first light”.

### 7.1.1. *Cryogenic System*

The first problem is our dewar. Our dewar is a recycled design from a dewar originally intended to hold liquid nitrogen for a mere 5 hours. With the redesign (by Mike Leung and Ian Ellwood), the dewar would hold LN for more than 40 hours when pumped down. However, this performance would not last. As time progressed, the LN would boil off quicker and quicker. When we pumped it down again, we found that the vacuum had decreased significantly, perhaps pointing to a leak in the dewar. However, a leak test performed by the Lab's vacuum shop indicated no leaks. Currently, we think the increase in pressure is due to outgassing of o-ring rubber inside the dewar, and we have yet to remedy this situation.

### 7.1.2. *Vibration*

Of more immediate concern than the dewar is that mechanical vibrations of the instrument translate to large output changes in the receiver. We can see noise that is synchronous with the rotation frequency even when the receiver input is terminated by  $50\Omega$ . In addition, merely stressing the beams up or down causes a change in the receiver's output. We think that the noise comes from stressing the SMA coaxial cables before the first amp. As the beams are stressed, they tilt, which exerts a force on the components inside the receiver. With the current design, it will be very difficult to deal with this noise.

## 8. **Looking to the Future**

Despite the fact that CMB RoPE is not even operational, we are already looking to the next generation of CMB polarimeters. Keeping the basic strategy intact, there are a number of ways to improve the instrument's performance.

The first issue to deal with would be the vibration. Due to the small diameter bearings we naively used, vibrations can easily live on the long beams. To effectively eliminate the vibrations, we could use a geared drive system on a ground-mounted circular track of comparable diameter to the beam length. By supporting the beams at the ends as well as the center, this would reduce the vibrations significantly.

Once the vibration issue is dealt with, then it becomes logical to look at the cryogenic system. The simplest remedy for our dewar problems is simply to fix our current dewar. However, this is not ideal since the use of such a simple dewar means the nitrogen must be refilled periodically, which means stopping the instrument and suspending data-taking while filling. The ideal solution would be a closed-cycle helium refrigerator which would cool the amplifier to 15 K. Not only would this provide drastically better noise performance, but it would also eliminate the periodic filling of liquid cryogenics. However, this would require a complete redesign of the first stage amplifier

system to take into account the new cooling system. In addition, closed-cycle refrigerators are very heavy, and mounting it on a rotating platform could prove troublesome. As an alternative to a 15 K system, 77 K systems are also available which are less expensive but obviously do not offer the noise benefits of a 15 K system.

The last logical upgrade is to change the frequency of operation. Because of galactic synchrotron foregrounds, it is preferable to work at a higher frequency range (due to the  $\nu^{-2.6}$  dependence of radiated synchrotron power). Observing at 30 GHz is a nice balance of getting above most of the galactic contamination while staying below dust emission and keeping atmospheric emission reasonable. Using a 30 GHz front end would require a 15 K cryogenic system due to the noise performance of current 30 GHz amplifiers at 77 K. In addition, the feedhorn would have to be redesigned since the current horn is designed for 9 GHz and is very wavelength-specific. The current warm RF section could still be utilized if the 30 GHz signal is mixed down to 9 GHz, but that would require an on-board local oscillator. Alternatively, we could keep the entire system at 30 GHz, which would require a completely new RF section. The dish we currently have is usable at 30 GHz, although with somewhat degraded performance.

## 9. Conclusion

Despite the many setbacks, CMB RoPE has made much progress since starting out with nearly nothing two years ago. If we regard CMB RoPE as a prototype for a next-generation CMB polarization experiment, it has been successful in elucidating the dos and don'ts of making a sensitive experiment. As a scientific endeavor, CMB RoPE might be called less than a success. As a learning experience, however, it has been outstanding.

## 10. Acknowledgments

I would like to thank Professor Smoot for giving me and my fellow students free rein to do things as we saw fit and learn from our (many) mistakes. In addition, I would like to thank John Gibson for his electronics help and Rich Kuiper for machine shop guidance. I would like to thank Ki Won Yoon, who was the impetus behind getting this project started and the driving force behind its progress. I would also like to thank Professor Mahiko Suzuki for helpful conversations when designing the feedhorn transition (I was enrolled in his electromagnetism class at the time). Finally, I would like to thank the many like-minded students who helped this project get to the point where it is today, in no particular order: Mike Leung, Mark Wong, Peter Curran, Ian Ellwood, Ben Larman, Raanan Bodzin, Abraham Harte, Meridith MacKnight, Erik Shirokoff, Nishanth Rajan, and James Lamb.



## REFERENCES

Alpher R.A., Bethe H.A., and Gamow G. *Phys. Rev.* **73**, 803, 1948

Penzias, A.D. and Wilson R.W., *Ap. J.* **142**, 419, 1965

Mather, J.C. et. al. *Ap. J.* **354**, L37, 1990

Smoot, G.F. et. al. *Ap. J.* **396**, L1, 1992

Kraus, J.D. *Radio Astronomy*. McGraw-Hill, New York, 1966.

Clarricoats, P.J.B. and Olver, A.D. *Corrugated Horns for Microwave Antennas*. Inspec, 1984.